Polymeric metal-containing ionic liquid sorbent coating for the determination of amines using headspace solid-phase microextraction

Kateryna Yavir[1], Philip Eor[2], Adam Kloskowski[1], Jared L. Anderson[2,*]

[1] Department of Physical Chemistry, Faculty of Chemistry, Gdansk University of Technology, Narutowicza Str. 11/12, Gdansk 80-233 Poland

[2] Department of Chemistry, Iowa State University, Ames, IA, 50011, USA

* Corresponding author. Department of Chemistry, Iowa State University, 1605 Gilman Hall, Ames, IA, 50011, USA. *E-mail address:* andersoj@iastate.edu (J.L. Anderson).

Abstract

This study describes the design, synthesis, and application of polymeric ionic liquid sorbent coatings featuring nickel metal centers for the determination of volatile and semi-volatile amines from water samples using headspace solid-phase microextraction. The examined polymeric ionic liquid sorbent coatings were composed of two ionic liquid monomers (tetra(3-vinylimidazolium)nickel bis[(trifluoromethyl)sulfonyl]imide $[Ni^{2+}(VIM)_4]\ 2[NTf_2^-]$ and 1-vinyl-3-hexylimidazolium $[HVIM^+][NTf_2^-]$), and an ionic liquid crosslinker (1,12-di(3-vinylimidazolium)dodecane $[(VIM)_2C_{12}^{2+}]\ 2[NTf_2^-]$). With these ionic liquid monomers and crosslinkers, three different types of coatings were prepared: PIL 1 based on the neat $[Ni^{2+}(VIM)_4]\ 2[NTf_2^-]$ monomer; PIL 2 consisting of the $[Ni^{2+}(VIM)_4]\ 2[NTf_2^-]$ monomer with addition of crosslinker, and PIL 3 comprised of the $[HVIM^+][NTf_2^-]$ monomer and crosslinker. Analytical performance of the prepared sorbent

Received: 14/02/2021; Revised: 19/04/2021; Accepted: 19/04/2021

This article has been accepted for publication and undergone full peer review but has not been through the copyediting, typesetting, pagination and proofreading process, which may lead to differences between this version and the Version of Record. Please cite this article as doi: 10.1002/jssc.202100119.

coatings using headspace solid-phase microextraction GC-MS was compared with the polydimethylsiloxane and polyacrylate commercial coatings. The PIL 2 sorbent coating yielded the highest enrichment factors ranging from 5500 to over 160000 for the target analytes. The developed headspace solid-phase microextraction GC-MS method was applied for the analysis of real samples (the concentration of amines was 200 μg L^{-1}), producing relative recovery values in the range of 90.9-120.0 % (PIL 1) and 83.0-122.7 % (PIL 2) from tap water, and 84.8-112.4 % (PIL 1) and 79.2-119.3 % (PIL 2) from lake water.

Keywords

Amines; polymeric metal-containing ionic liquids; nickel ions; solid-phase microextraction.

Article Related Abbreviations:

2,6-DTBP, 2,6-di-tert-butylpyridine; DAROCUR 1173, 2-hydroxy-2-methylpropiophenone; EF, enrichment factor; HS-SPME, headspace solid-phase microextraction; IL, ionic liquid; LLE, liquid-liquid extraction; MCILs, metal-containing ionic liquid; NaCl, sodium chloride; PA, polyacrylate; PDMS, polydimethylsiloxane; PIL, polymeric ionic liquid; R^2, coefficient of determination; RR, relative recovery; [HVIM$^+$][NTf$_2^-$], 1-vinyl-3-hexylimidazolium bis[(trifluoromethyl)sulfonyl]imide); [Ni^{2+}(VIM)$_4$] 2[NTf$_2^-$], tetra(3-vinylimidazolium)nickel bis[(trifluoromethyl)sulfonyl]imide; [(VIM)$_2$C$_{12}^{2+}$] 2[NTf$_2^-$], 1,12-di(3-vinylimidazolium)dodecane bis[(trifluoromethyl)sulfonyl]imide.

1. INTRODUCTION

Amines are well-known environmental pollutants that are widespread throughout the world. They can be released from a variety of anthropogenic (chemicals, pesticides, pharmaceuticals, automobiles, dyestuff, etc.) and natural sources (biomass burning, oceans, and vegetation) [1]. Amines are easily released to the environment through groundwater, rivers, lakes, and soil as well as industrial effluents or chemical decomposition products [2]. Most compounds of this class are hazardous and toxic to humans and animals. They can react with nitrosylating agents and, as a consequence, be converted to carcinogenic n-nitroamines [3]. Even though contamination of amines can exist in the environment at trace levels, they may have a mutagenic and toxic effect on animals and humans. Therefore, the concentration of amines in the surrounding water must be continuously monitored, and it is vital to find fast, easy, effective, and sensitive methods for their determination.

Solid-phase microextraction (SPME) is a solvent-free extraction technique and is an alternative to conventional extraction methods, such as liquid-liquid extraction (LLE) and solid-phase extraction (SPE) [4]. The procedure for extracting analytes from an aqueous solution using SPME consists of the following three main steps: a) exposing the fiber to the sample by direct-immersion (DI) or the headspace (HS) above the sample, b) absorbing/adsorbing the analytes by the sorbent, and c) desorption of the analytes from the coating by thermal or solvent extraction. The SPME method has become widely used to determine a wide range of analytes from complex matrices, such as samples of food products, biological substances, pharmaceuticals, and environmental samples [5-8]. SPME has numerous advantages over other extraction methods, such as being simple, rapid, easily automated, eliminates the use of toxic solvents, and allows for the collection of samples in-situ and in-vivo. One of the most important limitations of the method is the choice of commercially-available SPME sorbent coatings. Therefore, on-going research in the field is focused on developing new sorbent coatings that extend the range of analytes that can be effectively extracted. Various materials such as nanoparticles of noble metals, sorbents based on silica (silicon dioxide), ionogels, molecularly imprinted polymers, conductive polymers, carbon nanotubes, metal and/or metal oxide nanoparticles, graphene and graphene oxide, metal organic frameworks, ionic liquids (ILs), and polymeric ionic liquids (PILs) [9-17] hold promise due to their desired tunability. The above drawbacks are related to the general limitations of the SPME method. However, in the case of amine determination by SPME coupled to gas chromatography (GC), a number of additional problems arise due to their high aqueous solubility, volatility, polarity, and highly basic character (i.e., stronger sorption to polar stationary phases is observed with the decrease in the molecular mass of amines) [18].

ILs are a well-known group of materials that have been used as SPME sorbent coatings. These compounds consist of a bulky organic cation and a smaller inorganic/organic anion and are present as liquids below 100 °C. The physical and chemical properties of ILs are highly tunable based on selecting an appropriate anion and cation pair. When ILs are used as a polymerizable monomer, PILs are formed and retain many of the unique physico-chemical properties of ILs as well as additional advantages that include higher thermal and chemical stability, and a negligible change in viscosity when subjected to high temperatures [19, 20]. PILs have been used for the determination of various classes of analytes, including polycyclic aromatic hydrocarbons, fatty acid methyl esters, esters and benzene derivatives, carbon dioxide, estrogens, alcohols and amines, genotoxic or structurally alerting alkyl halides and aromatics, pyrethroids, and contaminants of emerging concern [10, 11, ~~16~~21].

Another interesting subclass of ILs is metal-containing ionic liquids (MCILs). MCILs are formed by incorporating transition and/or rare earth metals into their chemical structure [22]. In addition to possessing fundamental properties of ILs, the paramagnetic metals in MCILs impart magnetic, catalytic, and optical properties, which significantly increases the scope of their applications [23, 24]. MCILs have been used in various areas of analytical chemistry including extractions and microextractions, chromatographic separations, membrane applications and gas absorption, electrochemistry, and sensors [25, 26]. Incorporation of metal ions (Ni^{2+}, Mn^{2+}, Co^{2+}, Dy^{3+}, Gd^{3+}. Nd^{3+}) into the IL chemical structure significantly influences their interactions with analytes originating from different organic subclasses such as alcohols, ketones, chlorinated alkanes, aromatic compounds and amines [22, 27]. It has been observed that nickel-containing MCILs exhibit unique selectivity towards amines [27]. The viscosity of MCILs drop significantly with an increase of temperature, rendering them impractical in SPME. To overcome this obstacle, the creation of a polymerizable sorbent coating is required. A procedure using vinylimidazole ligands coordinated to silver ion and subsequent free radical polymerization to form a polymeric metal-containing ionic liquid was previously reported [28].

Using this approach, nickel-based PILs were synthesized in this study with or without the addition of crosslinker to investigate its effect on amine extraction performance. According to a previous study by Ho et al. [29], crosslinked PILs possess higher durability, stability, and robustness compared to linear PIL-based coatings. The effect of nickel cation in the PIL chemical structure was studied by further comparing the extraction performance to a structurally-similar PIL coating lacking the metal center. To benchmark the sorbent coatings, extractions of the targeted amine analytes were compared to commercially-available fibers consisting of PDMS and PA sorbent coatings. The developed HS-SPME-GC-MS method was finally applied for the analysis of real samples, including tap and lake water.

2. MATERIALS AND METHODS

2.1. Reagents and materials

The group of studied amines included pyridine (99.8 %), triallylamine (99.0 %), tripropylamine (≥ 98.0 %), 3-ethylpyridine (≥ 98.0 %), aniline (99.5 %), and 2,6-di-tert-butylpyridine (2,6-DTBP, ≥ 97.0 %), all purchased from Sigma-Aldrich (St. Louis, MO, USA). Table SM-1 of the supplementary material (SM) shows the structures and various physico-chemical properties of the analytes. Stock solutions of the individual analytes were prepared in acetonitrile (99.8 %, Sigma-Aldrich) at a concentration of 2000 mg L^{-1}. The intermediate solutions in acetonitrile were prepared by diluting the set of individual stock solutions to a level of 100 mg L^{-1} for each analyte. GC-MS calibration curves were obtained using a set of solutions prepared so that the volume of injected standard solutions were equal to 1 µL. Working solutions were prepared by spiking the intermediate solution into the ultrapure or real water samples containing sodium chloride (NaCl, ≥ 99.5 %, purchased from Fisher Scientific, Fair Lawn, NJ, USA). Ultrapure water (18.2 MΩ cm) was obtained from a Milli-Q water purification system (Millipore, Bedford, MA, USA).

For the synthesis of monomers and crosslinkers, the following reagents were used: 1-vinylimidazole (≥ 99.0 %), nickel(II) chloride (98.0 %), 1,12-dibromododecane (98.0 %), 1-bromohexane (98.0 %), all purchased from Sigma-Aldrich. Lithium bis[(trifluoromethyl)sulfonyl] imide ($LiNTf_2$) was acquired from SynQuest Laboratories (Alachua, FL, USA). The reagent 2-hydroxy-2-methylpropiophenone (> 96.0 %, DAROCUR 1173, Sigma-Aldrich) was used as an initiator in the polymerization reaction. Methanol (99.8 %), ethyl acetate (99.8 %), isopropanol (99.5 %), and dichloromethane (≥ 99.8 %) were purchased from Sigma-Aldrich.

The commercial SPME fibers, featuring polyacrylate (PA, 85 µm) and polydimethylsiloxane (PDMS, 100 µm) coatings, were provided as gifts from Millipore-Sigma. Elastic nitinol wires were used as solid supports in the preparation of the SPME fibers (Nitinol Devices & Components, Fremont, CA, USA). Blank SPME assemblies (24 Ga) were provided by Millipore-Sigma (Bellefonte, PA, USA).

Real water samples were collected from the laboratory tap in Ames (IA, USA) and from Lake LaVerne on the campus of Iowa State University, respectively. The samples were stored in the dark using glass bottles at 4 °C before use. Prior to analysis, NaCl was added to a concentration of 30 % (w/v).

2.2. Instrumentation

Amine separations were carried out using an Agilent Technologies 7890B GC equipped with a 5977A MS detector (single quadrupole) on a CP-Sil8 CB capillary column (length 30 m, 0.25 mm ID, 0.25 µm film thickness). Ultrapure helium was used as carrier gas at a flow rate of 1 mL min^{-1}. The inlet was operated in splitless mode with an inlet temperature of 190 °C. The following oven program was used: initial temperature equal to 40 °C, then the temperature was increased at 2 °C min^{-1} up to 80 °C, followed by an increase to 270 °C at 30 °C min^{-1}, and finally held for 1 min. The MS employed electron ionization (EI) at 70 eV and gain factor mode. The transfer line temperature was set at 250 °C, while the source and quadrupole temperatures were fixed at 230 °C and 150 °C, respectively. Data were acquired in single ion monitoring (SIM) mode. Identification of the amines was accomplished by considering the retention time, presence of quantifier and qualifier ions for each analyte (see Table SM-1 of SM), and the ratio between those ions. The peak area corresponding to the quantifier ion was used for quantitative purposes.

Scanning electron microscopy (SEM) images of the nickel-based PIL fibers were obtained using a FEI Quanta-250 microscope (FE-SEM).

2.3. Synthesis of ionic liquid monomers and crosslinker

Two IL monomers, namely, 1-vinyl-3-hexylimidazolium bis[(trifluoromethyl)sulfonyl]imide $[HVIM^+][NTf_2^-]$ and tetra(3-vinylimidazolium)nickel bis[(trifluoromethyl)sulfonyl]imide $[Ni^{2+}(VIM)_4]\ 2[NTf_2^-]$, as well as the 1,12-di(3-vinylimidazolium)dodecane bis[(trifluoromethyl)sulfonyl]imide $[(VIM)_2C_{12}^{2+}]\ 2[NTf_2^-]$ IL crosslinker were synthesized and used in the study.

The $[Ni^{2+}(VIM)_4]\ 2[NTf_2^-]$ IL monomer was synthesized using a modification of a previously published procedure [26]. One equivalent (millimolar) of anhydrous nickel (II) chloride was added to four equivalents of 1-vinylimidazole in methanol with stirring at room temperature overnight. After reaction, solvent was removed by rotary evaporation. The resulting solid material was dried under vacuum for 24 h at 40 °C. The obtained solid ($[Ni^{2+}(VIM)_4]\ 2[Cl^-]$) was then reacted with $LiNTf_2$ at a 1:4 molar ratio, respectively, in acetone and water by stirring at room temperature for 5 hours. The solvent was subsequently evaporated and the material dried under vacuum. After drying, the material was dissolved in dichloromethane, and remaining lithium chloride was removed by liquid-liquid extraction with ultrapure water. In the final step, dichloromethane was evaporated under vacuum for 24 h at 40 °C. Elemental analysis (CHN): Calculated % for $C_{24}H_{24}F_{12}N_{10}NiO_8S_4$, Calculated; C, 28.96; H, 2.43; N, 14.07; S, 12.88. Found; C, 34.56; H, 3.17; N, 13.85; S, 9.34.

The $[HVIM^+][NTf_2^-]$ IL monomer and $[(VIM)_2C_{12}^{2+}]\ 2[NTf_2^-]$ IL crosslinker were synthesized according to previously published methods [30, 31]. The monomer and crosslinker were characterized using ^1H NMR and electrospray ionization (ESI)-MS and spectra are shown in Figures SM 1-5 of the SM.

2.4. Preparation of solid-phase microextraction fibers

All coatings were prepared by on-fiber UV-initiated polymerization following previously described procedures [29]. The composition and mass ratio of components used for the preparation of the IL-based coatings are shown in Table 1 and Figure 1. Three types of coatings were prepared: PIL 1 consisting of pure $[Ni^{2+}(VIM)_4]\ 2[NTf_2^-]$ monomer; PIL 2 with monomer and $[(VIM)_2C_{12}^{2+}]\ 2[NTf_2^-]$ crosslinker, and PIL 3 based on the $[HVIM^+][NTf_2^-]$ monomer and crosslinker. The PIL3 coating was used as a reference to study the effect of Ni^{2+} metal center in the PIL on extraction performance. The IL monomer, IL crosslinker (if applied), and free radical initiator were mixed in appropriate proportions at 55 °C. The homogenous mixture was manually placed on the surface of a previously derivatized nitinol support. Derivatization of elastic nitinol wires was carried out according to a previously published method [32] and glued into a commercial SPME device. The coatings were exposed to UV irradiation (360 nm) for two hours to promote polymerization. Finally, the obtained fibers were thermally conditioned in the GC injection port at 200 °C for 30 min.

2.5. Headspace solid-phase microextraction procedure

Samples for HS-SPME were placed in 20 mL glass vials closed with open-top caps and polytetrafluoroethylene/silicone septa (Supelco). For all experiments, the sample volume was maintained at 10 mL. Before exposure of the SPME fiber, samples were thermostated at the temperature of extraction for 15 min using a hotplate with an accuracy of ± 0.5 °C. Subsequently, samples were spiked with required volumes of the stock solution and mixed at 800 rpm for 5 min. A Corning PC-420D magnetic stirring hotplate (Corning, NY, USA) and a stir bar (1 cm length × 0.5 cm diameter, Fisher Scientific) were used for mixing. The fiber was exposed to the headspace of the sample solution for 10-70 min at 25-70 °C. After extraction, the fibers were immediately inserted into the GC injection port for thermal desorption at 190 °C for 10 min. The temperature and desorption time were optimized in advance by studying carry-over effects.

The amino functional groups within amine molecules are responsible for strong and specific interactions with silane groups and siloxane bridges. Consequently, this leads to their strong retention, which often results in broad, asymmetrical chromatographic peaks and low sensitivity. To avoid these issues, it is necessary to choose an optimal GC column. The following capillary columns were examined to identify the most effective separation of amines: HP-5ms (30 m, 0.25 mm ID, 0.25 μm film thickness), DB-WAX (30 m, 0.25 mm ID, 0.25 μm film thickness), and CP-Sil8 CB (30 m, 0.25 mm ID, 0.25 μm film thickness). The CP-Sil8 CB column has demonstrated superior performance in amine separation and was selected for further studies.

3. RESULTS AND DISCUSSION

3.1. Characterization of nickel-based polymeric ionic liquid fibers

The introduction of transition metals into the IL chemical structure may significantly affect its interactions with organic compounds, thereby influencing extraction properties. This feature was exploited in the determination of phenolics, polycyclic aromatic hydrocarbon, insecticide compounds and lipophilic organic UV filters using MCILs in micro-liquid extraction techniques [33, 34]. More systematic studies evauating the selectivity of MCILs were performed by studying the retention of anaytes obtained from inverse gas chromatography when the MCIL is used as a stationary phase [27]. MCILs with anions containing metals (Ni^{2+}, Mn^{2+}, Co^{2+}, Dy^{3+}, Gd^{3+}. Nd^{3+}) with acetylacetonate ligands were investigated. The results indicated an exceptionally high affinity of amines (especially pyridine) for nickel-containing MCILs. However, due to their liquid state, these compounds cannot be directly applied as extraction phases in SPME. In this study, the structural features of the MCIL were modified by incorporating 1-vinylimidazole ligands featuring terminal double bonds that can be polymerized while exploiting the amine function of the ligand to coordinate to the nickel metal ion. A similar approach has been used successfully to produce UV curable SPME PIL coatings featuring silver ion for the selective extraction of unsaturated compounds [28].

In the current study, the following three types of SPME sorbent coatings were prepared: (1) polymerized neat $[Ni^{2+}(VIM)_4][NTf_2^-]$ monomer (PIL 1), (2) $[Ni^{2+}(VIM)_4][NTf_2^-]$ monomer with the addition of 50 % w/w of $[(VIM)_2C_{12}^{2+}][NTf_2^-]$ as crosslinker (PIL 2), and

(3) $[HVIM^+][NTf_2^-]$ monomer and a crosslinker (PIL 3). The goal was to investigate the effect of added crosslinker (PIL 1 vs. PIL 2) and the presence of nickel cation (PIL 2 vs. PIL 3) on the extraction performance for a variety of amines. The chemical structures and physical properties of the fiber coatings are shown in Table 1.

As the analytes should be released from the fiber by thermal desorption, the thermal stability of PIL sorbent coating is very important. The fibers were tested by exposure to the GC inlet. All PIL fibers were stable up to 200 °C. In comparison, non-polymerized ILs with the same anion and containing Ni^{2+} ion showed significantly lower decomposition temperatures of 164 and 178 °C, respectively [22]. It can be concluded that the increased thermal resistance in the tested coatings results from the formation of a stable polymer structure [35].

The visual appearance, thickness, and regularity of the developed nickel-based PIL sorbent coatings were evaluated using scanning electron microscopy (SEM). Figure 2 shows the images of fibers with and without added crosslinker.

3.2. Optimization of the extraction procedure

When optimizing extraction methods in SPME, the most important parameters are extraction and desorption times, sampling and desorption temperatures, salt concentration, and sample agitation. In the case of compounds that dissociate in aqueous solutions, sample solution pH should also be taken into account.

Amines are weak bases and can undergo hydrolysis in aqueous solutions. To facilitate their transfer to the headspace, they must remain undissociated. Thus, the pH of the aqueous samples must be adjusted accordingly. The pKa values describing acidity of protonated amines are listed in Table SM-1. Tripropylamine lies at the upper limit with a pKa equal to 10.58. According to the general rule of equilibrium, it is widely accepted that keeping the pH of the solution two units above the pKa value of analytes ensures its quantitative presence in the neutral form [36]. Therefore, the pH of the aqueous solution was increased by the addition of a strong base (NaOH) to 13.

The values of some parameters mentioned above were assumed *a priori*. The thermal desorption temperature of the analytes should permit their quickest possible transfer to the chromatographic column. Typically, the limitation is the thermal stability of the sorbent material and analytes. Based on the previously determined durability of the fibers (approximately 200 °C), it was assumed that analytes could still be desorbed at a slightly lower temperature of 190 °C.

The optimal time for thermal desorption was determined using a pre-determined temperature of the GC injection port. For optimization purposes, extraction of analytes using the tested fibers was carried out from samples using a concentration two times higher than the planned working range (i.e., 400 μg L^{-1}). The desorption studies were carried out using times ranging from 2 to 20 minutes. The longest desorption time of 10 min was required for PIL 1 to avoid carry-over effects. To ensure uniform conditions for all investigated fibers, the identical desorption time was applied in all further experiments.

Stirring using a magnetic stir bar was utilized as the sample agitation method. It is well-known that increasing agitation of the sample is often accompanied by an increase in the mass transfer caused by convection [5]. In this study, the highest stirring speed was limited by the formation of droplets of samples on the fiber surfaces caused by too vigorous agitation. Thus, as optimal stir rate of 800 rpm was used for all experiments in the study.

3.2.1. Influence of salt content

Previous HS-SPME studies reported that the addition of salts can affect the extraction efficiency due to the salting out effect [37]. The interaction of water with these additional ions may have a significant impact on the extraction process as their solubility in water can be expected to increase or decrease. Amines may be particularly susceptible to the salting out effect [5]. Since the change in solubility of analytes in water is related to the sample-headspace equilibrium, the salting out effect was investigated with fibers containing the PIL 1 and PIL 2 sorbent coatings. Aqueous samples that did not contain NaCl yielded very low extraction efficiency and high experimental error (RSD > 15 %). Hence, NaCl concentrations of 5, 15, and 30 % (w/v) were evaluated at 40 °C with an extraction time of 30 min. The obtained results are shown in Figure SM-6. The results indicate that in the case of the tested amines, the addition of salt significantly reduced their solubility in water and increased their extraction efficiency from the headspace. The most pronounced effect was observed for pyridine using PIL 1 where the chromatographic peak area increased by 44-fold; in contrast, the extraction efficiency for 2,6-DTBP using PIL 2 increased only by 2-fold. For the analyzed analytes, the effect of NaCl addition was qualitatively and quantitatively similar for both PIL 1 and PIL 2. Based on obtained results, solutions with a concentration of 30 % (w/v) were chosen for further experiments.

3.2.2. Influence of extraction temperature

It is known that an increase in the extraction temperature often leads to an increase in the diffusion coefficient, thereby increasing the rate of mass transfer to the headspace [5]. The effect of extraction temperature on the extraction efficiency was investigated in the temperature range from 25 to 70 °C (in 15 °C increments) for 30 min using 30 % (w/v) NaCl in the aqueous sample solution. The obtained extraction temperature profiles are shown in Figure SM-7 of SM. In the case of the HS mode, an equilibrium is formed for the analyte between the aqueous solution, headspace, and sorbent coating. Partitioning of the analytes between the solution and the fiber depends on the values of the partition coefficients between the sample and the headspace as well as the headspace and fiber coating. As can be observed, the extraction efficiency evolves with increasing temperature in four ways: reaches a maximum (3-ethylpyridine, pyridine), decreases (triallylamine, 2,6-DTBP), increases (tripropylamine), and remains constant (aniline). Increasing extraction temperature may also impede analyte absorption on sorbents because of it being an exothermic process [38]. A decreasing trend in extraction efficiency for volatile analytes (i.e., triallylamine, 2,6-DTBP, and pyridine) at higher temperatures is likely due to their absorption on PIL sorbents being more hindered compared to the case of less volatile analytes at the given conditions. The profiles obtained for both fibers (PIL 1 and PIL 2) follow a similar trend, except for tripropylamine, where in the case of the crosslinked sorbent coating the extraction efficiency increases significantly with temperature. A compromised temperature condition of 45 °C was identified and chosen for all amines.

3.2.3. Influence of extraction time

The optimal extraction time was determined by analyzing the analyte extraction efficiency upon exposing the fiber to the sample headspace at times varying from 10 to 70 minutes using an extraction temperature of 45 °C and 30 % (w/v) NaCl in the aqueous sample solution. Figure SM-8 of SM shows the effect of extraction time on the extraction efficiency of PIL 1 and PIL 2 sorbent coatings. It can be observed that for different analytes, various trends were obtained. For aniline and 2,6-DTBP, the extraction efficiency did not change significantly when extraction times longer than 10 min were tested. Pyridine, tripropylamine, and 3-ethylpyridine were more efficiently extracted at longer extraction times, while a drop in extraction efficiency occurred for triallylamine.

There is no single physico-chemical property that explains the differences in time profiles obtained for different analytes as the most volatile analyte (pyridine) does not reach equilibrium in the tested time range, while the least volatile 2,6-DTBP undergoes equilibration after 10 min. Also, it could be expected that for compounds with higher values of the enrichment factor their transport within the fiber coating will require an extended equlibration time. Meanwhile, triallylamine shows even a slight decrease in extraction efficiency in PIL 2 with time, while the less efficiently extracted tripropylamine is far from equilibrium. In determining the optimal extraction time, the compounds that did not reach equilibrium within the studied time (tripropylamine, 3-ethylpyridine, and pyridine) were taken into account. For those compounds, extending the extraction time from 50 to 70 minutes increased the sum of chromatographic peaks areas by less than 20 %. Thus, in further studies, an extraction time of 50 minutes was used for all fibers.

3.3. Analytical performance of the developed headspace solid-phase microextraction method and evaluation of extraction efficiency

Partial validation of the HS-SPME method utilizing the PIL and commercial fibers involved determination of coefficient of determination (R^2), limits of detection (LOD), limits of quantification (LOQ), repeatability (relative standard deviation, RSD), and relative recovery (RR). The working ranges for all amines and each of the investigated SPME fibers are presented in Table SM-2. A working range from 5 to 200 μg L^{-1} was used for the studied PIL and commercial fibers. For all fibers within the working range, satisfactory linearity with the R^2 values above 0.990 was found (see Table SM-2 of SM). Table SM-3 shows the sensitivities of the methods expressed by the calibration slope for each fiber. In the case of most amines (with the exception of 2,6-DTBP), the nickel-based fibers (PIL 1 and PIL 2) exhibited higher sensitivity than commercial fibers and the PIL 3 fiber.

The LODs were calculated on the basis of a signal-to-noise ratio of three, and the LOQs as ten times the above-mentioned ratio. The LOD values of 2,6-DTBP for all fibers were significantly lower compared to other amines with a maximum of 0.0037 μg L^{-1} for PIL 1 and a minimum of 0.000077 μg L^{-1} for PIL 2. LODs of the other amines ranged from 0.05-1.56 μg L^{-1} for PIL 1, 0.02 to 0.84 μg L^{-1} for PIL 2, 0.01-1.41 μg L^{-1} for PIL 3, 1.02-12.76 μg L^{-1} for PA, and 0.08-6.48 μg L^{-1} for PDMS (Table 2). LODs of pyridine, triallylamine, tripropylamine, and aniline obtained with the PIL-based SPME method were similar to or lower than the LOD values measured with other analytical methods such as capillary electrophoresis, GC-MS, and dispersive liquid-liquid microextraction coupled with GC-MS, which ranged from 0.07 to 42 μg L^{-1} [39-42]. The LOQ values for all fibers are shown in Table SM-4 of SM.

The repeatability of the methods was calculated by performing triplicate extractions of aqueous samples spiked with amines at a concentration 200 μg L^{-1}, and are presented in Table 2. The RSD values for PIL fibers did not exceed 15 % for all analytes and are comparable with those obtained using commercial fibers. Relative recovery was calculated as the ratio of the concentrations of spiked solutions to its value determined in the course of the analytical procedure. Calculated RR values are summarized in Table SM-5 of SM. The RRs ranged from 84.5 to 116.3 % for all fibers, proving the usefulness of the PIL fibers in analytical applications. The performance of each type of PIL fiber began to decrease after ~70 extraction/desorption cycles. Therefore, 60 cycles was selected as the optimal lifetime of the sorbent coatings.

In addition, a comparison was made between the extraction efficiency of the developed nickel-based PIL fibers and selected commercial fibers (PA and 100 μm PDMS) using the enrichment factor (EF) [43]. This parameter is a suitable tool for comparing the extraction ability by considering the nature of the sorption coatings of fibers, regardless of its geometrical dimensions. The EF parameter was calculated as the ratio of the analyte concentration in the fiber and the analyte concentration in the aqueous sample. The obtained values of EFs are shown in Table SM-6 and represented in Figure 3 . An example chromatogram is shown in Figure SM-9 of SM. The EF values for both nickel-based PIL fibers (PIL 1 and PIL 2) are higher than those obtained for the both commercial fibers (PA and PDMS) and standard PIL fiber (PIL 3) in the case of all target analytes, with the exception of 2,6-DTBP for the PIL 1 fiber. For most analytes, the EF values of PIL 2 were higher than PIL 1. This is due to the increased surface area of the crosslinked PIL 2 resulting in enhanced analyte-sorbent interactions [44, 45]. Therefore, the PIL 2 fiber was most suitable for the extraction of amines by HS-SPME in this work. This sorbent coating may be a particularly attractive alternative to commercially-available coatings for the determination of volatile amines.

3.4. Analysis of real samples

Lake and tap water were analyzed to evaluate the matrix effect of environmental samples on the performance of the developed nickel-based PIL fibers and the HS-SPME-GC-MS method for the determination of amines. The water samples were spiked with amines at a concentration of 200 μg L^{-1} and extracted under optimal conditions using the PIL 1 and PIL 2 fibers. The matrix effect was evaluated in terms of relative recovery and repeatability (Table 3). The RRs of lake water ranged from 84.8 to 112.4 % for PIL 1 and from 79.2 to 119.3 % for PIL 2. For spiked tap water samples, the RRs varied between 90.9-120.0 % for PIL 1 and 83.0-122.7 % for PIL 2. The obtained RSD values for both fibers and both types of water samples were acceptable and were less than 15 %. Based on both parameters, no significant matrix effects were identified.

4. CONCLUSIONS

In this work, two nickel-based PIL sorbent coatings were successfully developed and applied in HS-SPME coupled to GC-MS for the determination of volatile and semi-volatile amines, including pyridine, triallylamine, tripropylamine, 3-ethylpyridine, aniline, and 2,6-DTBP, from water samples. After optimizing the extraction parameters, the extraction efficiency of the developed fibers (PIL 1 and PIL 2) was evaluated and compared with commercial fibers using the EF normalization parameter. The nature of the nickel-based sorbent coatings provided higher efficiencies than the conventional PIL coating as well as commercial PA and PDMS coatings for all of the analytes studied.

Additionally, the results from this study show that the analytical performance of the nickel-based PIL, PA, and PDMS (100 μm) fibers were comparable in terms of working range, coefficient of determination, LOD, LOQ, reproducibility, and RR. Low LODs were achieved for developed fibers, and ranged from 0.003717 to 1.56 mg L^{-1} and from 0.000077 to 0.84 μg L^{-1} for PIL 1 and PIL 2, respectively. Finally, the developed HS-SPME-GC-MS method was applied for the analysis of real samples, including tap and lake water. The RRs of PIL 2 ranged from 83.0 to 122.7 % for tap water and from 79.2 to 119.3 % for lake water.

ACKNOWLEDGMENTS

J.L.A. acknowledges funding from the Chemical Measurement and Imaging Program at the National Science Foundation (Grant No. CHE-1709372). Kateryna Yavir acknowledges the development of an interdisciplinary Ph.D. program with an international dimension (InterPhD II, POWR.03.02.00-IP.08-00-DOK/16) for the funding provided to carry out the following research.

CONFLICT OF INTEREST

The authors have declared no conflict of interest.

REFERENCES

[1] Kataoka H., Derivatization reactions for the determination of amines by gas chromatography and their applications in environmental analysis. *J. Chromatogr. A* 1996, *733*, 19–34.

[2] Zhu Y., Wang M. H., Du H. Y., Wang F., Mou S. F., Haddad P. R., Organic analysis by ion chromatography: 1. Determination of aromatic amines and aromatic diisocyanates by cation-exchange chromatography with amperometric detection. *J. Chromatogr. A* 2002, *956*, 215–220.

[3] Chung K. T., Mutagenicity and carcinogenicity of aromatic amines metabolically produced from azo dyes. *Environ. Carcino. & Ecotox. Revs.* 2000, *C18*~~(1)~~, 51–74.

[4] Arthur C. L., Pawliszyn J., Solid phase microextraction with thermal desorption using fused silica optical fibers. *Anal. Chem.* 1990, *62*, 2145–2148.

[5] Pawliszyn J., Handbook of Solid Phase Microextraction. Elsevier, Waltham, MA, USA 2012.

[6] Kataoka H., Lord H. L., Pawliszyn J., Applications of solid-phase microextraction in food analysis. *J. Chromatogr. A* 2000, *880*, 35–62.

[7] Chary N. S., Fernandez-Alba A. R., Determination of volatile organic compounds in drinking and environmental waters. *Trends Anal. Chem.* 2012, *32*, 60–75.

[8] Snow N. H., Solid-phase micro-extraction of drugs from biological matrices. *J. Chromatogr. A* 2000, *885*, 445–455.

[9] Hashemi B., Zohrabi P., Shamsipur M., Recent developments and applications of different sorbents for SPE and SPME from biological samples. *Talanta* 2018, *187*, 337–347.

[10] Yu H., Ho T. D., Anderson J. L., Ionic liquid and polymeric ionic liquid coatings in solid-phase microextraction. *Trends Anal. Chem.* 2013, *45*, 219–232.

[11] Patinha D. J., Silvestre A. J., Marrucho I. M., Poly (ionic liquids) in solid phase microextraction: Recent advances and perspectives. *Prog. Polym. Sci.* 2019, *98*, 101148.

[12] Yavir K., Marcinkowski Ł., Marcinkowska R., Namieśnik J., Kloskowski A., Analytical applications and physicochemical properties of ionic liquid-based hybrid materials: A review. *Anal. Chim. Acta* 2019, 1054, 1–16.

[13] Gutiérrez-Serpa, A., Rocío-Bautista P., Pino V., Jiménez-Moreno F., Jiménez-Abizanda, A. I., Gold nanoparticles based solid-phase microextraction coatings for determining organochlorine pesticides in aqueous environmental samples. *J. Sep. Sci.* 2017, *40*, 2009–2021.

[14] Luo Z., Chen G., Li X., Wang L., Shu H., Cui X., Chang C., Zeng A., Fu Q., Molecularly imprinted polymer solid-phase microextraction coupled with ultra high performance liquid chromatography and tandem mass spectrometry for rapid analysis of pyrrolizidine alkaloids in herbal medicine. *J. Sep. Sci.* 2019, *42*, 3352–3362.

[15] Li G., Row K., Ternary deep eutectic solvent magnetic molecularly imprinted polymers for the dispersive magnetic solid-phase microextraction of green tea. *J. Sep. Sci.* 2018, *41*, 3424–3431.

[16] Wan Ibrahim W. N., Sanagi M. M., Mohamad Hanapi N. S., Kamaruzaman S., Yahaya N., Wan Ibrahim W. A., Solid-phase microextraction based on an agarose-chitosan-multiwalled carbon nanotube composite film combined with HPLC–UV for the determination of nonsteroidal anti-inflammatory drugs in aqueous samples. *J. Sep. Sci.* 2018, *41*, 2942–2951.

[17] Abolghasemi M. M., Yousefi V., Piryaei M., Synthesis of a metal–organic framework confined in periodic mesoporous silica with enhanced hydrostability as a novel fiber coating for solid-phase microextraction. *J. Sep. Sci.* 2015, *38*, 1187–1193.

[18] Zeeuw J., Vonk N., Buyten J., Heijnsdijk P., Clarisse R., The Analysis of Volatile Amines by Capillary Gas Chromatography. Varian, Middelburg, Netherlands 2000.

[19] Qian W., Texter J., Yan F., Frontiers in poly(ionic liquid)s: syntheses and applications. *Chem. Soc. Rev.* 2017, *46*, 1124–1159.

[20] Yuan J., Mecerreyes D., Antonietti M., Poly(ionic liquid)s: an update. *Prog. Polym. Sci.* 2013, *38*, 1009-1036.

[21] Mei M., Huang X., Chen L., Recent development and applications of poly (ionic liquid)s in microextraction techniques. *Trends Anal. Chem.* 2019, *112*, 123–134.

[22] Chand D., Farooq M. Q., Pathak A. K., Li J., Smith E. A., Anderson J. L., Magnetic ionic liquids based on transition metal complexes with N-alkylimidazole ligands. *New J. Chem.* 2019, *43~~(1)~~*, 20–23.

[23] Santos E., Albo J., Irabien A., Magnetic ionic liquids: synthesis, properties and applications. *RSC Adv.* 2014, *4*, 40008–40018.

[24] Wang H., Yan R., Li Z., Zhang X., Zhang S., Fe-containing magnetic ionic liquid as an effective catalyst for the glycolysis of poly (ethylene terephthalate). *Catal. Commun.* 2010, *11*, 763–767.

[25] Sajid M., Magnetic ionic liquids in analytical sample preparation: a literature review. *Trends Anal. Chem.* 2019, *113*, 210–223.

[26] Clark K. D., Nacham O., Purslow J. A., Pierson S. A., Anderson J. L., Magnetic ionic liquids in analytical chemistry: a review. *Anal. Chim. Acta.* 2016, *934*, 9–21.

[27] Nan H., Peterson L., Anderson J. L., Evaluating the solvation properties of metal-containing ionic liquids using the solvation parameter model. *Anal. Bioanal. Chem.* 2018, *410~~(19)~~*, 4597–4606.

[28] Trujillo-Rodríguez M. J., Anderson J. L., Silver-based polymeric ionic liquid sorbent coatings for solid-phase microextraction: Materials for the selective extraction of unsaturated compounds. *Anal. Chim. Acta* 2019, *1047*, 52–61.

[29] Ho T. D., Yu H., Cole W. T., Anderson J. L., Ultraviolet photoinitiated on-fiber copolymerization of ionic liquid sorbent coatings for headspace and direct immersion solid-phase microextraction. *Anal. Chem.* 2012, *84*, 9520–9528.

[30] Anderson J. L., Armstrong D. W., Immobilized ionic liquids as high-selectivity/high-temperature/high-stability gas chromatography stationary phases. *Anal. Chem.* 2005, *77*, 6453–6462.

[31] Anderson J. L., Ding R., Ellern A., Armstrong D. W., Structure and properties of high stability geminal dicationic ionic liquids. *J. Am. Chem. Soc.* 2005, *127*, 593–604.

[32] Ho T. D., Toledo B. R., Hantao L. W., Anderson J. L., Chemical immobilization of crosslinked polymeric ionic liquids on nitinol wires produces highly robust sorbent coatings for solid-phase microextraction. *Anal. Chim. Acta* 2014, *843*, 18–26.

[33] Yu H., Merib J., Anderson J. L., Faster dispersive liquid–iquid microextraction methods using magnetic ionic liquids as solvents. *J. Chromatogr. A* 2016, *1463*, 11–19.

[34] Chisvert A., Benedé J. L., Anderson J. L., Pierson S. A., Salvador A., Introducing a new and rapid microextraction approach based on magnetic ionic liquids: Stir bar dispersive liquid microextraction. *Anal. Chim. Acta* 2017, *983*, 130–140.

[35] Pierson S. A., Nacham O., Clark K. D., Nan H., Mudryk Y., Anderson J. L., Synthesis and characterization of low viscosity hexafluoroacetylacetonate-based hydrophobic magnetic ionic liquids. *New J. Chem.* 2017, *41*, 5498–5505.

[36] Sarafraz-Yazdi A., Ardaki M. S., Amiri A., Determination of monocyclic aromatic amines using headspace solid-phase microextraction based on sol–gel technique prior to GC. *J. Sep. Sci.* 2013, *36*, 1629–1635.

[37] Vila M., Celeiro M., Lamas J. P., Dagnac T., Llompart M., Garcia-Jares C., Determination of fourteen UV filters in bathing water by headspace solid-phase microextraction and gas chromatography-tandem mass spectrometry. *Anal. Methods* 2016, *8*, 7069–7079.

[38] Sarafraz-Yazdi A., Vatani H., A solid phase microextraction coating based on ionic liquid sol–gel technique for determination of benzene, toluene, ethylbenzene and o-xylene in water samples using gas chromatography flame ionization detector. *J. Chromatogr. A* 2013, *1300*, 104–111.

[39] Hattori T., Okamura H., Asaoka S., Fukushi K., Capillary zone electrophoresis determination of aniline and pyridine in sewage samples using transient isotachophoresis with a system-induced terminator. *J. Chromatogr. A* 2017, *1511*, 132–137.

[40] Liu, S., Wang W., Chen J., Sun J., Determination of aniline and its derivatives in environmental water by capillary electrophoresis with on-Line concentration. *Int. J. Mol. Sci.* 2012, *13*, 6863–6872.

[41] Tsukioka T., Ozawa H., Murakami T., Gas chromatographic-mass spectrometric determination of lower aliphatic tertiary amines in environmental samples. *J. Chromatogr. A* 1993, *642*, 395–400.

[42] Diao C. P., Wei C. H., Rapid determination of anilines in water samples by dispersive liquid–liquid microextraction based on solidification of floating organic drop prior to gas chromatography–mass spectrometry. *Anal. Bioanal. Chem.* 2012, *403*, 877-884.

[43] Pena-Pereira F., Marcinkowski Ł., Kloskowski A., Namieśnik J., Silica-based ionogels: nanoconfined ionic liquid-rich fibers for headspace solid-phase microextraction coupled with gas chromatography–barrier discharge ionization detection. *Anal. Chem.* 2014, *86*, 11640–11648.

[44] Trujillo-Rodríguez M. J., Nan H., Anderson J. L., Expanding the use of polymeric ionic liquids in headspace solid-phase microextraction: Determination of ultraviolet filters in water samples. *J. Chromatogr. A* 2018, *1540*, 11–20.

[45] Ho T. D., Yu H., Cole W. T. S., Anderson J. L., Ultraviolet photoinitiated on-fiber copolymerization of ionic liquid sorbent coatings for headspace and direct immersion solid-phase microextraction. *Anal. Chem.* 2012, *84*, 9520–9528.

SUPPORTING INFORMATION

Additional supporting information may be found online in the Supporting Information section at the end of the article.

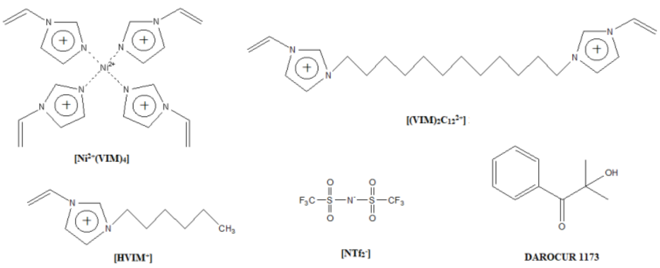

FIGURE LEGENDS

Figure 1. Chemical structures of the cations, anion, and UV initiator (DAROCUR 1173) used for the preparation of sorbent coatings investigated in this study.

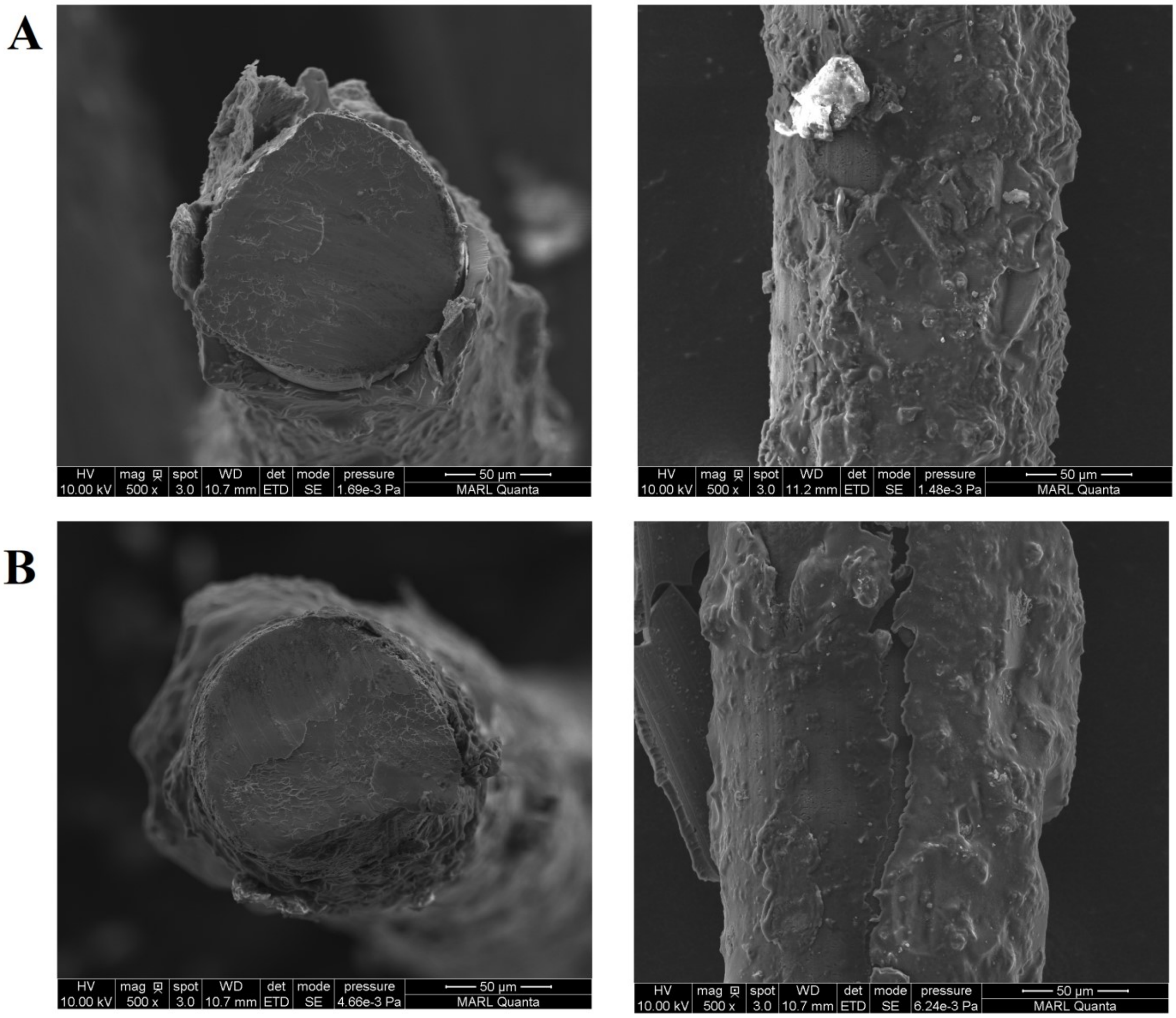

Figure 2. Scanning electron microscopy (SEM) images of the nickel-based PIL fibers examined in this study: PIL 1 (500×) ≈ 8±1.3 µm (A) and PIL 2 (500×) ≈ 11±1.9 µm (B).

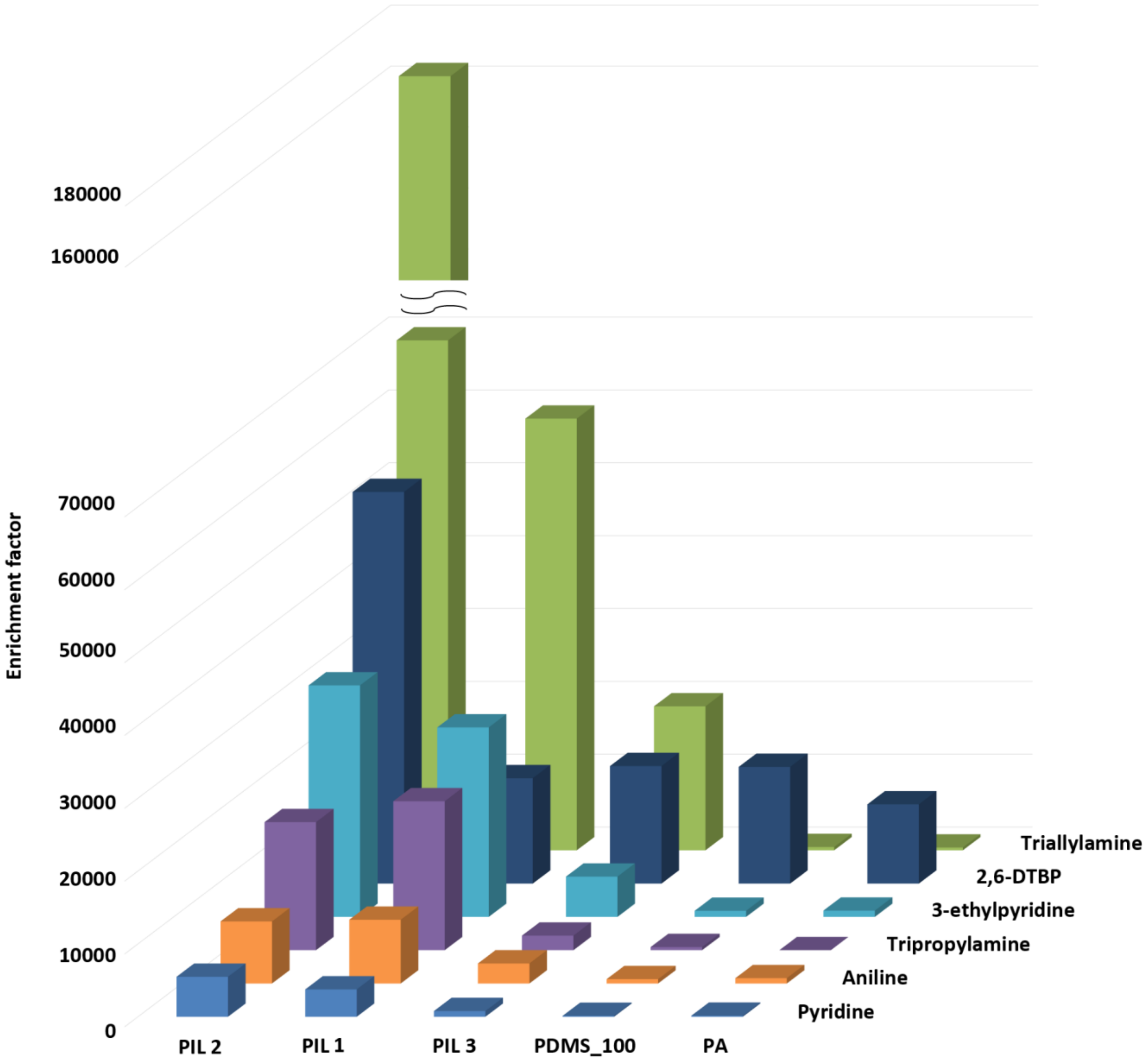

Figure 3. Enrichment factors calculated for the studied amines using five different SPME fibers featuring highly varied sorbent coating chemistries.

TABLE LEGENDS

Table 1. Composition of sorbent coatings and dimensions of fibers examined in this study.

PIL fiber abbreviation [a]	**IL monomer**	**IL crosslinker** [b]	**Film thickness ± SD (µm)** [c]	**Volume (µL)**
PIL 1	$[Ni^{2+}(VIM)_4]\ 2[NTf_2^-]$	-	~ 8 ± 1.3	0.043
PIL 2	$[Ni^{2+}(VIM)_4]\ 2[NTf_2^-]$	$[(VIM)_2C_{12}^{2+}]\ 2[NTf_2^-]$	~ 11 ± 1.9	0.063
PIL 3	$[HVIM^+][NTf_2^-]$	$[(VIM)_2C_{12}^{2+}]\ 2[NTf_2^-]$	~ 22 ± 3.8	0.146

[a] DAROCUR 1173 was used as a UV initiator for all fibers (50 % w/w, respect to the monomer).

[b] 50 % w/w, respect to the monomer.

[c] Estimated from Scanning Electron Microscopy (SEM) images (the length of fibers were 1.35 cm).

Table 2. Limits of detection (LOD, signal-to-noise ratio = 3) and relative standard deviation (RSD) obtained for amines when performing HS-SPME-GC-MS using different SPME fibers. LOD determined using samples spiked to 5 and 50 µg L^{-1}. RSD calculated using results obtained for samples with a concentration of analytes equal 200 µg L^{-1}.

Analyte	**LOD [a], µg L^{-1}**					**RSD [d], % (n = 3)**				
	PIL 1	**PIL 2**	**PIL 3**	**PDMS_100**	**PA [b]**	**PIL 1**	**PIL 2**	**PIL 3**	**PDMS_100**	**PA**
Pyridine	0.70	0.22	1.41	0.56	7.21	7.9	5.2	13.4	7.8	13.6
Triallylamine	0.28	0.03	0.01	0.08	3.19	11.1	13.4	14.7	6.0	11.9
Tripropylamine	0.24	0.02	0.04	0.27	n.d. [c]	14.7	4.3	11.9	6.2	n.d.
3-ethylpyridine	0.05	0.09	0.78	0.30	1.02	12.6	7.7	10.3	2.6	5.9
Aniline	1.56	0.84	1.11	6.48 [b]	1.82	8.8	14.0	13.9	5.8	6.2
2,6-DTBP	0.003717	0.000077	0.000295	0.000022	0.000072	13.9	13.6	13.1	10.8	11.4

[a] 5 µg L^{-1} – the spiked concentration of amines.

[b] 50 µg L^{-1} – the spiked concentration of amines.

[c] n.d. – not detected.

[d] 200 µg L^{-1} – the spiked concentration of amines.

Table 3. Analysis of lake and tap water using the HS-SPME-GC-MS method with nickel-based PIL fibers.

Analyte	PIL 1				PIL 2			
	Lake water		Tap water		Lake water		Tap water	
	RR (%)	RSD (%)	RR (%)	RSD (%)	RR (%)	RSD (%)	RR (%)	RSD (%)
Pyridine	112.4	3.0	99.3	12.1	119.3	8.2	105.6	5.0
Triallylamine	99.4	10.9	118.9	11.4	82.5	12.9	122.2	4.8
Tripropylamine	87.7	5.5	120.0	6.0	98.3	5.7	98.3	9.7
3-ethylpyridine	108.3	12.9	90.9	6.7	118.7	8.4	122.7	4.2
Aniline	111.9	6.2	107.3	12.5	91.0	14.0	93.8	10.5
2,6-DTBP	84.8	10.9	114.1	10.0	79.2	8.5	83.0	12.4